Contributions to Discrete Mathematics

Volume 11, Number 2, Pages 79–101
ISSN 1715-0868

A CLASS OF SPHERICAL FOLDING SUBDIVISIONS

CATARINA P. AVELINO AND ALTINO F. SANTOS

Abstract. The classification of the dihedral folding tessellations of the sphere whose prototiles are a kite and an equilateral or isosceles triangle was obtained in recent papers by C.P. Avelino and A.F. Santos. In this paper we extend this classification to scalene triangles by presenting all the dihedral folding tessellations of the sphere by kites and scalene triangles in which the longest side of the kite is equal to the shorter side of the triangle.

1. Introduction

By a *folding tessellation* or *folding tiling* of the sphere S^2, we mean an edge-to-edge pattern of spherical geodesic polygons that fills the whole sphere with no gaps and no overlaps such that the "underlying graph" has even valency at any vertex, and the sums of alternate angles around each vertex are π.

Folding tilings (f-tilings, for short) are strongly related to the theory of isometric foldings on Riemannian manifolds. In fact, the set of singularities of any isometric folding corresponds to a folding tiling; see [**?**] for the foundations of this subject.

The study of these special class of tessellations was initiated in [**?**] with a complete classification of all spherical monohedral folding tilings. Ten years later, in [**?**], Ueno and Agaoka established the complete classification of all triangular spherical monohedral tilings without any restriction on angles.

Dawson has also been interested in special classes of spherical tilings; see [**?**], [**?**] and [**?**], for example.

The complete classification of all spherical f-tilings by rhombi and triangles was obtained in 2005 in [**?**]. A detailed study of the triangular spherical folding tilings by equilateral and isosceles triangles is presented in [**?**].

Spherical f-tilings by two non congruent classes of isosceles triangles have recently been obtained [**?**].

Received by the editors November 24, 2015, and in revised form Marth 16, 2016.

2010 *Mathematics Subject Classification.* Primary: 52C20; Secondary: 52B05, 20B35.

Key words and phrases. dihedral f-tilings, combinatorial properties, spherical trigonometry, symmetry groups.

This research was partially supported by Fundação para a Ciência e a Tecnologia (FCT) through projects UID/MAT/00013/2013 and UID/Multi/04621/2013.

The classification of dihedral folding tilings by kites and equilateral or isosceles triangles was obtained recently; see [**?**], [**?**], [**?**], and [**?**] for details. In this paper we initiate the classification of dihedral folding tilings of the sphere by kites and scalene triangles: in particular, we shall obtain all the dihedral f-tilings of the sphere by kites and scalene triangles in which the longest side of the kite is equal to the shorter side of the triangle. Our goal is to obtain all the spherical f-tilings by any kite and any triangle.

A spherical kite K (cf. Figure 1-I) is a spherical quadrangle with two pairs of congruent adjacent sides such that not all four sides are congruent. Let us denote by $\alpha_1, \alpha_2, \alpha_1, \alpha_3$, with $\alpha_2 > \alpha_3$, the internal angles of K in cyclic order. The side lengths are denoted by a and b and satisfy $a < b$. Henceforth in this paper, T denotes a spherical scalene triangle with internal angles $\beta > \gamma > \delta$ and length sides $c > d > e$; see Figure 1-II.

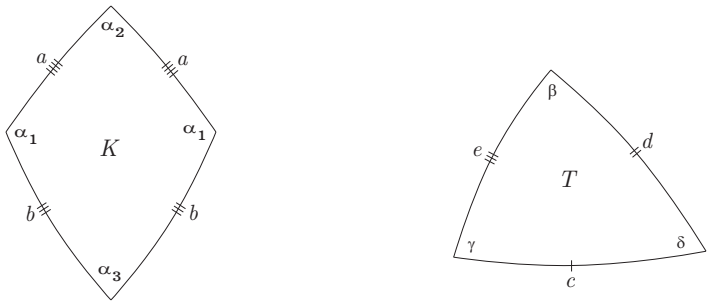

FIGURE 1. A spherical kite K and a spherical scalene triangle T.

Taking into account the area of the prototiles K and T, we have that

$$2\alpha_1 + \alpha_2 + \alpha_3 > 2\pi \quad \text{and} \quad \beta + \gamma + \delta > \pi.$$

Moreover, since $\alpha_2 > \alpha_3$ we also have

$$\alpha_1 + \alpha_2 > \pi.$$

After certain initial assumptions are made, it is usually possible to deduce sequentially the nature and orientation of most of the other tiles in a potential f-tiling. Eventually, either a complete tiling is crafted, or an impossible configuration, proving that the hypothetical tiling fails to exist, is reached. In the diagrams that follow, the order in which these deductions can be made is indicated by the numbering of the tiles. For $j \geq 2$, the location of tiling j can be deduced directly from the configurations of tiles $1, 2, \ldots, j-1$, and from the hypothesis that the configuration is part of a complete tiling, except where otherwise indicated.

We begin by pointing out that any f-tiling using K and T has at least two cells congruent to K and T, respectively, such that the cells are in adjacent positions in exactly one of the situations illustrated in Figure 2.

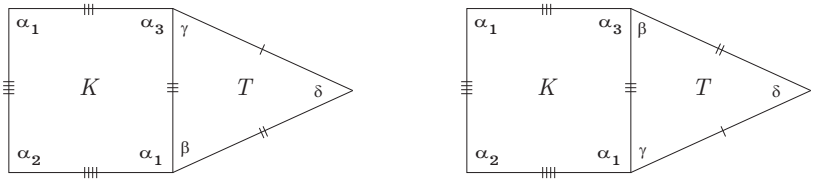

FIGURE 2. Distinct cases of adjacency.

Using spherical trigonometric formulas with $b = e$, we obtain

$$\frac{\cos\delta + \cos\beta\cos\gamma}{\sin\beta\sin\gamma} = \frac{\cos\frac{\alpha_2}{2} + \cos\alpha_1\,\cos\frac{\alpha_3}{2}}{\sin\alpha_1\,\sin\frac{\alpha_3}{2}}. \tag{1.1}$$

2. Case of Adjacency I

Suppose that any f-tiling using K and T has at least two cells congruent, respectively, to K and T, such that the cells are in adjacent positions as illustrated in Figure 2-I. By considering the internal angles of the kite K, we find that we have necessarily one of the following situations:

$$\alpha_1 \geq \alpha_2 > \alpha_3 \quad \text{or} \quad \alpha_2 > \alpha_1, \alpha_3;$$

note that these include the cases in which $\alpha_2 > \alpha_1 \geq \alpha_3$ and $\alpha_2 > \alpha_3 > \alpha_1$.

The two propositions that follow address these distinct cases.

Proposition 2.1. *If $\alpha_1 \geq \alpha_2 > \alpha_3$, then there is an f-tiling using K and T if and only if*

$$\alpha_1 + \beta = \pi, \quad \alpha_2 = \frac{\pi}{2}, \quad 2\gamma + \alpha_3 = \pi, \quad \textit{and} \quad \delta = \frac{\pi}{3}.$$

In this situation, there exists a continuous family of f-tilings, say $\mathcal{U}_\beta$, with $\beta \in (\beta_{\min}, \beta_{\max})$, where

$$\beta_{\min} = \arccos\sqrt{\frac{2}{11}} \approx 64.76^\circ$$

and

$$\beta_{\max} = \arccos\frac{\sqrt{6}-1}{4} \approx 68.75^\circ.$$

A planar and a 3D representation of $\mathcal{U}_\beta$ are given in Figure 9 and Figure 11-II, respectively.

Proof. Suppose that any f-tiling using K and T has at least two cells congruent, respectively, to K and T, such that the cells are in adjacent positions as illustrated in Figure 2-I with $\alpha_1 \geq \alpha_2 > \alpha_3$ and $\alpha_1 > \pi/2$.

There cannot be two angles α_3 in adjacent positions. In fact, it is enough to take into account the edge lengths of the prototiles and observe that $2\alpha_1 \geq \alpha_1 + \alpha_2 > \pi$; see Figure 3-I.

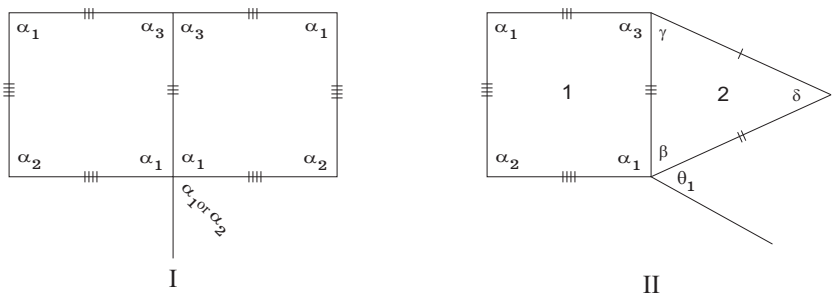

FIGURE 3. Local configurations

It then follows that, with the labeling of Figure 3-II, we have

$$\theta_1 = \beta \qquad \text{or} \qquad \theta_1 = \delta.$$

This leads us to consider two cases:

CASE 1: $\theta_1 = \beta$:

Suppose firstly that $\theta_1 = \beta$. Then we have necessarily that $\alpha_1 + \beta = \pi$ or $\alpha_1 + \beta < \pi$.

SUBCASE 1.1: $\alpha_1 + \beta = \pi$:

If $\alpha_1 + \beta = \pi$, then since $\alpha_1 > \pi/2 > \beta$, we obtain the local configuration illustrated in Figure 4-I. From this we conclude that $\alpha_2 \leq \pi/2$. If $\alpha_2 < \frac{\pi}{2}$, we get $2\alpha_2 + k\alpha_3 = \pi$ for some $k \geq 1$ (cf. Figure 4-II). Analyzing the side lengths of K and T, we find that the other sum of alternate angles must contain $\alpha_1 + \alpha_2$, which is greater than π, and leads us to a contradiction. Therefore $\alpha_2 = \pi/2$. Summarizing, we have that

$$\alpha_1 > \alpha_2 = \frac{\pi}{2} > \beta > \gamma > \delta\,, \quad \alpha_2 > \alpha_3, \quad \text{and} \quad \gamma + \delta > \frac{\pi}{2}.$$

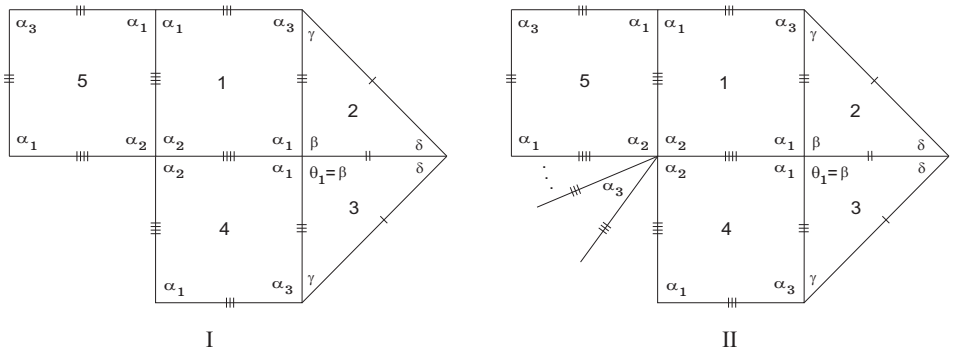

FIGURE 4. Local configurations

Suppose now the configuration illustrated in Figure 5-I. With the labeling of this figure, we must have

$$\theta_2 = \gamma \qquad \text{or} \qquad \theta_2 = \beta \qquad \text{or} \qquad \theta_2 = \alpha_3.$$

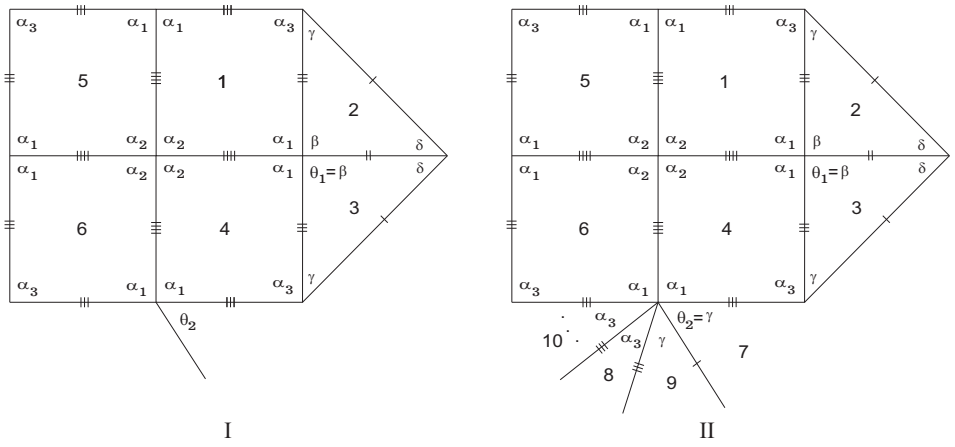

FIGURE 5. Local configurations

SUBCASE 1.1.1: $\theta_2 = \gamma$:
Suppose that $\theta_2 = \gamma$. Then we have $\alpha_1 + \gamma < \alpha_1 + \beta = \pi$, so by the previous relation between angles we get $\alpha_1 + \gamma + k\alpha_3 = \pi$ for some $k \geq 1$ (cf. Figure 5-II). The configuration forces the appearance of (at least) two angles α_3 in adjacent positions, leading us to a contradiction as seen in Figure 3-I.

SUBCASE 1.1.2: $\theta_2 = \beta$:
Assume now that $\theta_2 = \beta$. Then we obtain the local configuration illustrated in Figure 6-I, where the vertex v has valency greater than four.

SUBCASE 1.1.2.1: v HAS VALENCY SIX:
Let us suppose firstly that v is a vertex of valency six. Then, we easily conclude that $2\gamma + \alpha_3 = \pi$, leading us to the configuration of Figure 6-II. Taking into account the area of the dark triangle, composed by tiles 9, 10, and 11, we see that $\alpha_2 + 2\delta - \pi > 0$, which means that $\delta > \pi/4$.

The next two tiles adjacent to tile 9, say 12 and 13, must be kites. As $\alpha_1 + \alpha_2 > \pi$, they are completely determined as shown in Figure 7.

Now, the angle labeled by x cannot be γ as seen in Subcase 1.1.1. On the other hand, if $x = \alpha_3$, then in an adjacent vertex we would obtain $\alpha_1 + \gamma < \pi < \alpha_1 + \gamma + \rho$, for all $\rho \in \{\alpha_1, \alpha_2, \alpha_3, \beta, \gamma, \delta\}$, which is not possible. Therefore $x = \beta$ and we get the configuration represented in Figure 8.

Since $\delta > \pi/4$, we have $3\delta = \pi$ or $3\delta + k\alpha_3 = \pi$ for some $k \geq 1$. However, the second situation cannot occur by an analysis of the side lengths; thus we obtain $\delta = \frac{\pi}{3}$. More precisely, one has that

$$\alpha_1 > \alpha_2 > \beta > \gamma > \delta > \alpha_3$$

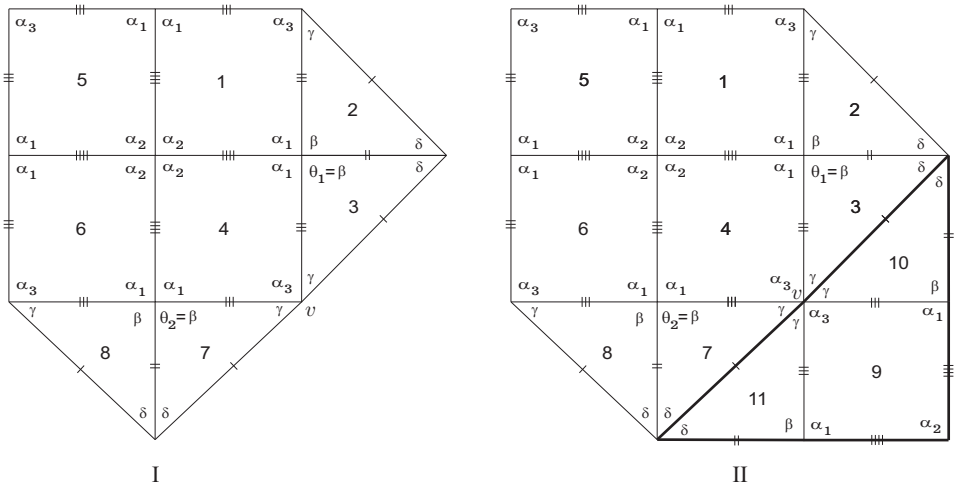

FIGURE 6. Local configurations

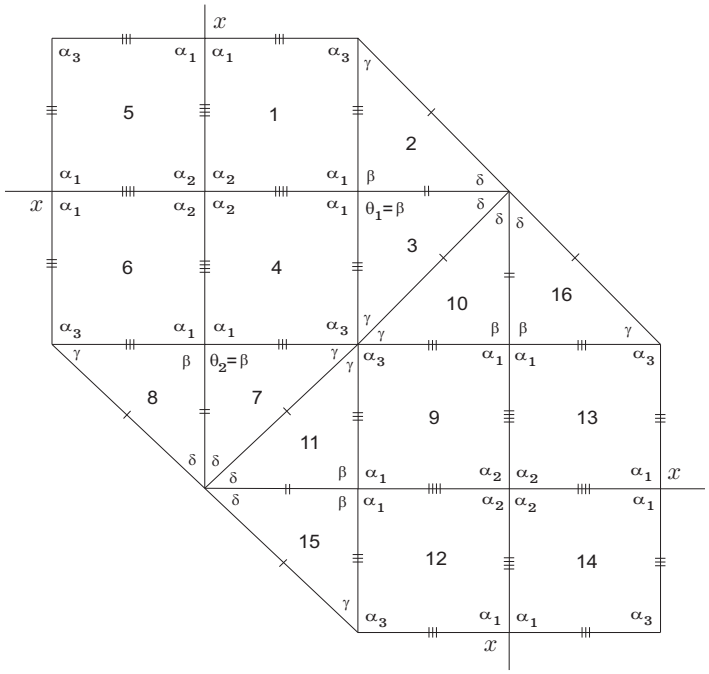

FIGURE 7. Local configuration

with $\alpha_2 = \pi/2$, $\delta = \pi/3$, $\alpha_1 + \beta = \pi$ and $2\gamma + \alpha_3 = \pi$.

The last configuration extends now in a unique way to obtain the one illustrated in Figure 9. Such a local configuration is limited by a great circle

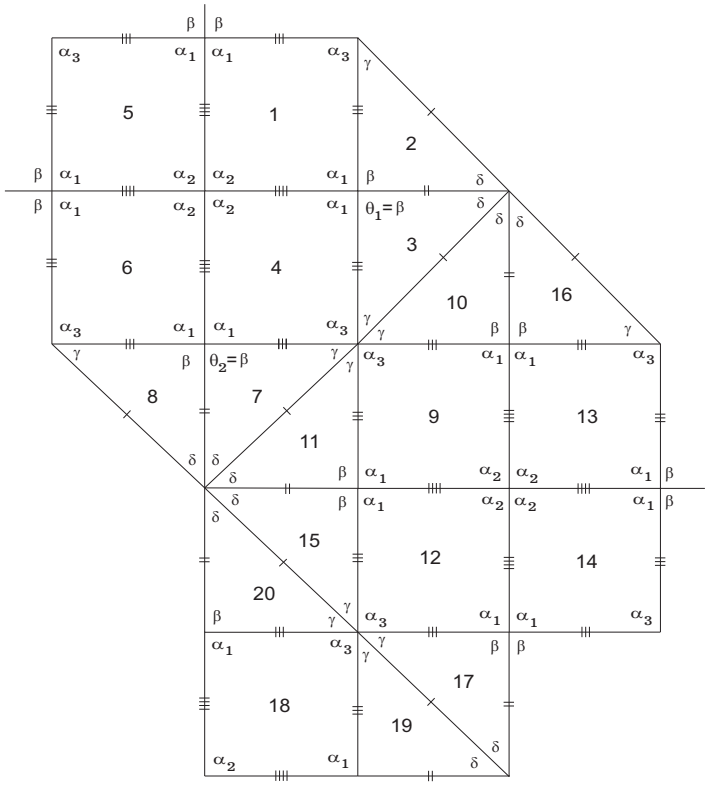

FIGURE 8. Local configuration

(the dark closed line), and it corresponds to one half of a spherical f-tiling, with the other half being obtained by reflection in the equator.

Analyzing Figure 9, we get $a+c+d = \pi/2$. Upon considering the distinct types of vertices, we have

$$\alpha_1 + \beta = \pi \text{ (24 vertices)}, \quad 2\,\alpha_2 = \pi \text{ (6 vertices)},$$

$$2\gamma + \alpha_3 = \pi \text{ (12 vertices)}, \quad \text{and} \quad 3\,\delta = \pi \text{ (8 vertices)}.$$

While considering the angles α_1, β, γ, and α_3, we see that we have two connection conditions to analyze; adding the relation given in Equation (1.1) shows that one degree of freedom still remains. In order to determine these angles and the interval of variation, we proceed as follows: the knowledge of α_2 and δ determines completely the side lengths of the extended triangle $(\pi/22, \pi/3, \pi/3)$ as union of tiles 9, 10, and 11, for instance; see Figure 10.

Using spherical trigonometry formulas we derive that

$$2\,c = 2\,\arccos\frac{\sqrt{6}}{3} = \arccos\frac{1}{3} \quad \text{and} \quad a + d = \arccos\frac{\sqrt{3}}{3}.$$

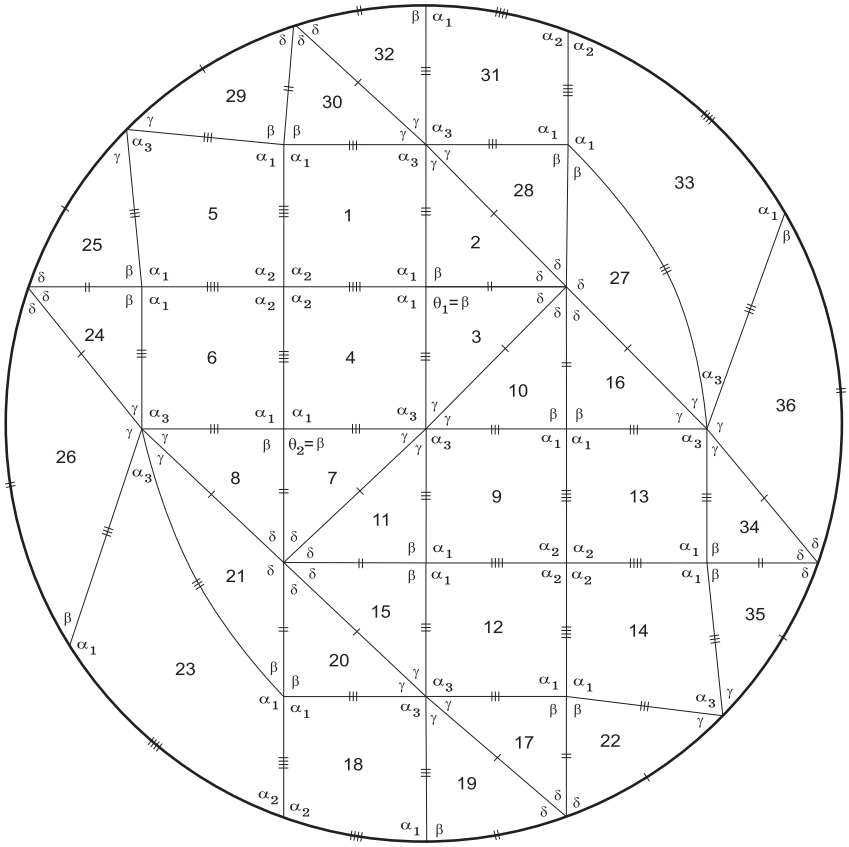

FIGURE 9. Half of a tiling

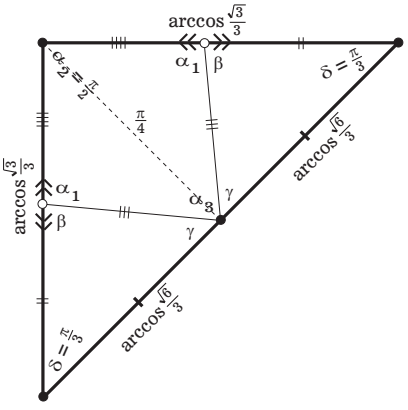

FIGURE 10. An extended triangle

Ignoring the edges of dimension $b = e$, this three-tile configuration can be substituted for each instance of the prototile of $\mathcal{U}$, obtained by Breda in [**?**]; see Figure 11-I.

It is easy to verify that adding edges joining the midpoint of the longest side to any point in the side of length $a + d$ of the extended triangle and making an angle $\beta \in (\pi/4, 2\pi/3)$ between them, we obtain an f-tiling, $\mathcal{U}_\beta$, as illustrated in Figure 11-II. Moreover, the choice of β determines completely α_1, γ, and α_3. However, the variation of β should be smaller, imposed by the restrictions on angles in this paper. Thus, the angle β must vary in an interval of the form $(\beta_{\min}, \beta_{\max})$.

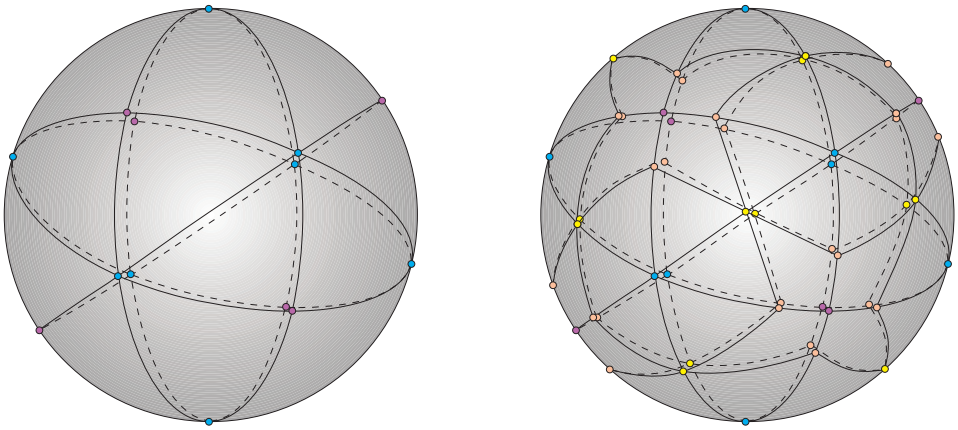

I II

FIGURE 11. 3D representations of $\mathcal{U}$ and $\mathcal{U}_\beta$, respectively

In order to determine $\beta_{\max}$ it is enough to make $\gamma = \frac{\pi}{3}$ so that

$$\cos\beta_{\max} = -\cos^2\frac{\pi}{3} + \sin^2\frac{\pi}{3}\cos\left(\arccos\frac{\sqrt{6}}{3}\right) = \frac{\sqrt{6}-1}{4}.$$

Therefore,

$$\beta_{\max} = \arccos\frac{\sqrt{6}-1}{4} \approx 68.75^\circ.$$

To determine $\beta_{\min}$ we consider the isosceles spherical triangle illustrated in Figure 12, obtained from $\beta = \gamma$.

One then has

$$\cos e = \cos^2\left(\arccos\frac{\sqrt{6}}{3}\right) + \sin^2\left(\arccos\frac{\sqrt{6}}{3}\right)\cos\frac{\pi}{3} = \frac{5}{6},$$

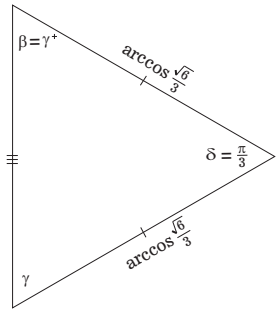

FIGURE 12. An isosceles spherical triangle

which means that $e = \arccos(5/6)$. We then obtain

$$\cos\beta_{\min} = \cos\gamma = \frac{\cos\left(\arccos\frac{\sqrt{6}}{3}\right) - \cos\left(\arccos\frac{\sqrt{6}}{3}\right)\cos\left(\arccos\frac{5}{6}\right)}{\sin\left(\arccos\frac{\sqrt{6}}{3}\right)\sin\left(\arccos\frac{5}{6}\right)} = \sqrt{\frac{2}{11}}$$

and so $\beta_{\min} = \arccos\sqrt{2/11} \approx 64.76°$.

SUBCASE 1.1.2.2: v HAS VALENCY GREATER THAN SIX:
Suppose now that v is a vertex of valency greater than six (Figure 6-I). Since $\beta < \pi/2$, we have $2\gamma + 2\delta > \pi$, as $\beta + \gamma + \delta > \pi$. Therefore, in the sum of alternate angles $\gamma + \gamma + \ldots$, there must be at most one angle δ, while the remaining angles are α_3. However, as illustrated in Figure 3-I, we cannot have two angles α_3 in adjacent positions. Thus, at vertex v we must have $3\gamma + \alpha_3 = \pi$ or $2\gamma + \delta + \alpha_3 = \pi$.

If $3\gamma + \alpha_3 = \pi$, then we obtain $\alpha_1 + \gamma + \alpha_3 < \pi$, since $\alpha_1 + \beta = \pi$ and $\beta + 2\gamma > \pi$. Now, because $2\alpha_1 + \alpha_2 + \alpha_3 > 2\pi$, we conclude that $\alpha_2 > 2\gamma + \alpha_3$, which is not possible as $\gamma > \pi/4$.

The case $2\gamma + \delta + \alpha_3 = \pi$ is illustrated in Figure 13-I; by symmetry, the order by angles α_3 and δ appears does not matter.

Now, with the labeling of Figure 13-II, if $x = \beta$ or $x = \gamma$, then $x + \beta < \pi$ and so $x + \beta + k\alpha_3 = \pi$ for some $k \geq 1$. Taking into account the side lengths, we will get two angles α_3 in adjacent positions, which leads to an impossible configuration (cf. Figure 3-I). Note that we also have $x \neq \alpha_3$. In fact, if $x = \alpha_3$, the case considered in Figure 13-II, we obtain, in an adjacent vertex, $\rho + \gamma + \delta > \beta + \gamma + \delta > \pi$ since ρ must be α_1 or α_2 (by analyzing the edge lengths).

By the analysis considered, we must have $x = \alpha_1$ leading us to the configuration illustrated in Figure 14. Now, the bold line delimits a spherical quadrilateral of internal angles $(\alpha_2, \delta, \alpha_2, \delta)$. This allows us to conclude that $2\alpha_2 + 2\delta - 2\pi > 0$, i.e., $\delta > \pi/2$, which is an impossibility.

SUBCASE 1.1.3: $\theta_2 = \alpha_3$:
Suppose finally that $\theta_2 = \alpha_3$ (cf. Figure 5-I). Such information leads to a vertex surrounded by the cyclic sequence $(\alpha_1, \alpha_3, \gamma, \ldots)$ as illustrated in

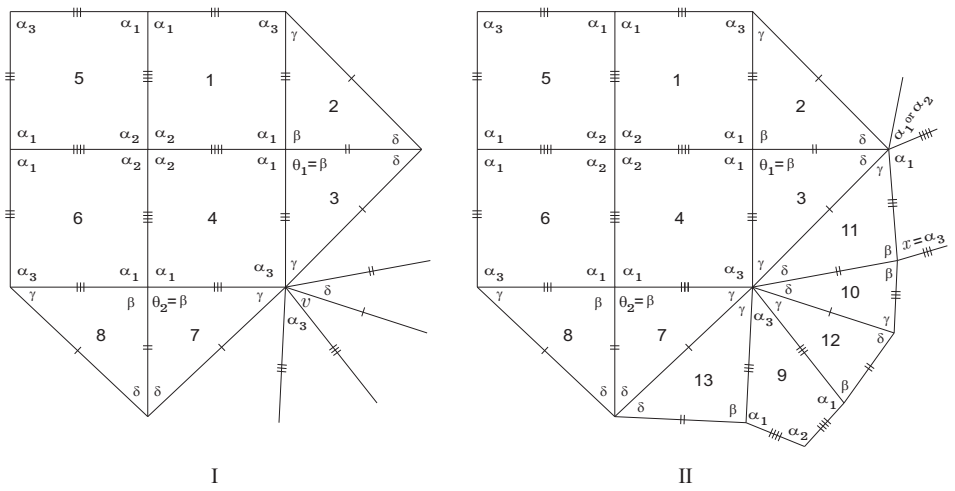

FIGURE 13. Local configurations

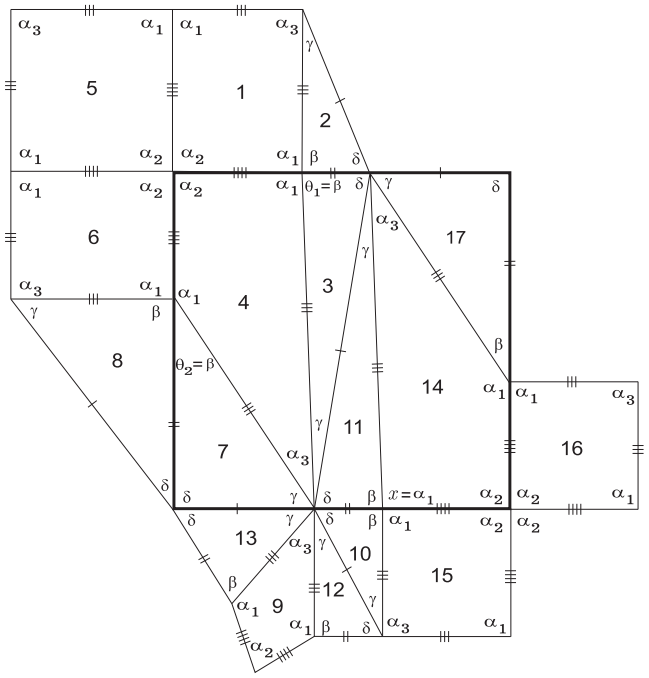

FIGURE 14. Local configuration

Figure 15-I. It follows that the sum of alternate angles containing α_1 and γ must be of the form $\alpha_1 + \gamma + k\alpha_3 = \pi$. Moreover, k must be equal to 1,

since we cannot have two angles α_3 in adjacent positions. This leads us to the configuration of Figure 15-II.

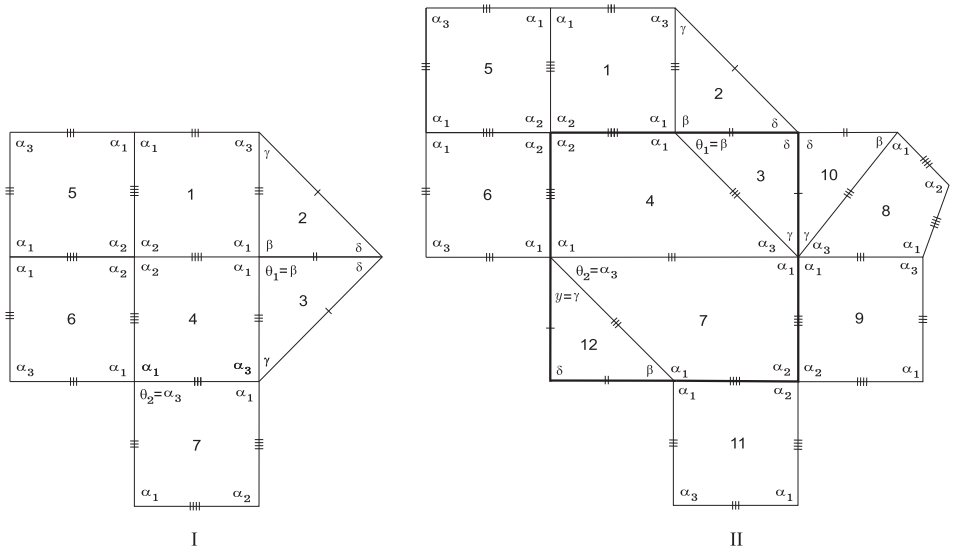

FIGURE 15. Local configurations

With the notation used in this figure, it is a straightforward exercise to show that $y \neq \alpha_1$, $y \neq \beta$ and $y \neq \alpha_3$, which gives $y = \gamma$. Once more, the spherical quadrilateral $\{3, 4, 7, 12\}$ (inside the dark line) has internal angles $(\alpha_2, \delta, \alpha_2, \delta)$. As $\alpha_2 = \pi/2$, we obtain $\delta > \pi/2$, leading us to a contradiction.

SUBCASE 1.2: $\theta_1 = \beta$:
Assume now that $\theta_1 = \beta$ (cf. Figure 3-II) and $\alpha_1 + \beta < \pi$ so that $\alpha_1 > \pi/2 > \beta$. In this situation, we must have $\alpha_1 + \beta + \alpha_3 = \pi$; see Figure 16-I. Taking into account the side lengths, we have no way to avoid two angles α_3 in adjacent positions, which is impossible.

CASE 2: $\theta_1 = \delta$:
Suppose now that $\theta_1 = \delta$ (cf. Figure 3-II). Then we have necessarily $\alpha_1 + \delta = \pi$ or $\alpha_1 + \delta < \pi$.

SUBCASE 2.1: $\alpha_1 + \delta = \pi$:
If $\alpha_1 + \delta = \pi$, analyzing the side lengths shows that we have no way to complete the sum of alternate angles containing β (cf. Figure 16-II).

SUBCASE 2.2: $\alpha_1 + \delta < \pi$:
Finally, suppose that $\alpha_1 + \delta < \pi$. It is easy to verify that none of the angles α_1, α_2, and β can be included in the sum of alternate angles containing α_1 and δ. On the other hand, if γ appears in the alternating sum $\alpha_1 + \delta + \ldots = \pi$, then $\beta > \alpha_1$ and so β can only add to α_3 and δ. However, this is not possible by considering the edge lengths. Thus we are led to conclude that $\alpha_1 + \delta + k_1\delta + k_2\alpha_3 = \pi$ for some positive integers k_1 and k_2 with $k_1 + k_2 > 0$.

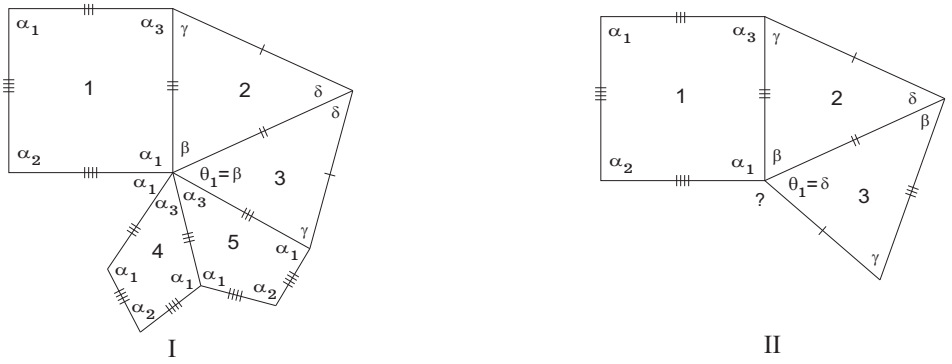

FIGURE 16. Local configurations

Observe that if $k_1 = 0$, then the sum of alternate angles containing β would be greater than or equal to $\beta + \alpha_1 + \gamma > \pi$, which is not possible. On the other hand, if $k_2 = 0$, then by considering the side lengths we obtain an impossibility as well.

Thus we conclude that $k_1 \geq 1$ and $k_2 = 1$, as two adjacent angles of α_3 are not allowed; this situation is illustrated in Figure 17. Once again it follows that the sum of alternate angles containing β is $\beta + \alpha_1 + \gamma + \cdots > \pi$, which is an impossibility.

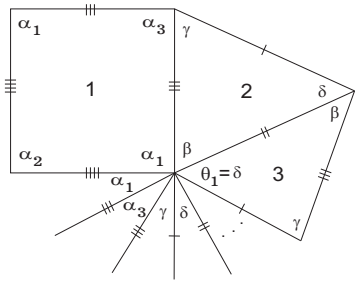

FIGURE 17. Local configuration

□

Proposition 2.2. *If $\alpha_2 > \alpha_1, \alpha_3$, then there is no f-tiling using K and T.*

Proof. Suppose that any f-tiling using K and T has at least two cells congruent, respectively, to K and T, such that the cells are in adjacent positions as illustrated in Figure 2-I and $\alpha_2 > \alpha_1, \alpha_3$ with $\alpha_2 > \pi/2$.

We claim that there cannot be two angles α_2 in adjacent positions (cf. Figure 18-I). In fact, it is enough to take into account the edge lengths of the prototiles and observe that $2\,\alpha_2 \geq \alpha_2 + \alpha_1 > \pi$.

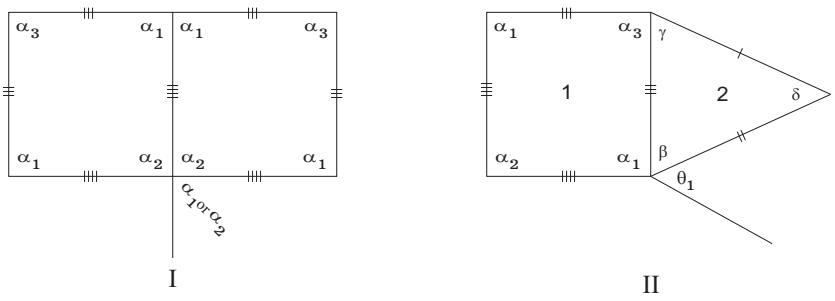

FIGURE 18. Local configurations

It then follows that, with the labeling of Figure 18-II, we necessarily have

$$\theta_1 = \beta \qquad \text{or} \qquad \theta_1 = \delta.$$

This leads us to consider the following cases:

CASE 1: $\theta_1 = \beta$:

Suppose firstly that $\theta_1 = \beta$. Then we must have $\alpha_1 + \beta = \pi$ or $\alpha_1 + \beta < \pi$.

SUBCASE 1.1: $\alpha_1 + \beta = \pi$:

If $\alpha_1 + \beta = \pi$, we get the local configuration presented in Figure 19-I, where two angles α_2 cannot be avoided.

SUBCASE 1.2: $\alpha_1 + \beta < \pi$: Suppose now that $\alpha_1 + \beta < \pi$. We shall distinguish the cases

$$\alpha_1 \geq \alpha_3 \qquad \text{and} \qquad \alpha_3 > \alpha_1.$$

SUBCASE 1.2.1: $\alpha_1 \geq \alpha_3$

Assume firstly that $\alpha_1 \geq \alpha_3$, i.e., $\alpha_2 > \alpha_1 \geq \alpha_3$. If, in addition, $\alpha_1 \geq \gamma$, then we must have $\alpha_1 + \beta + k\alpha_3 = \pi$ for some $k \geq 1$, as illustrated in Figure 19-II. Once more we obtain two angles α_2 in adjacent positions (as forced by the side lengths), leading us to a contradiction.

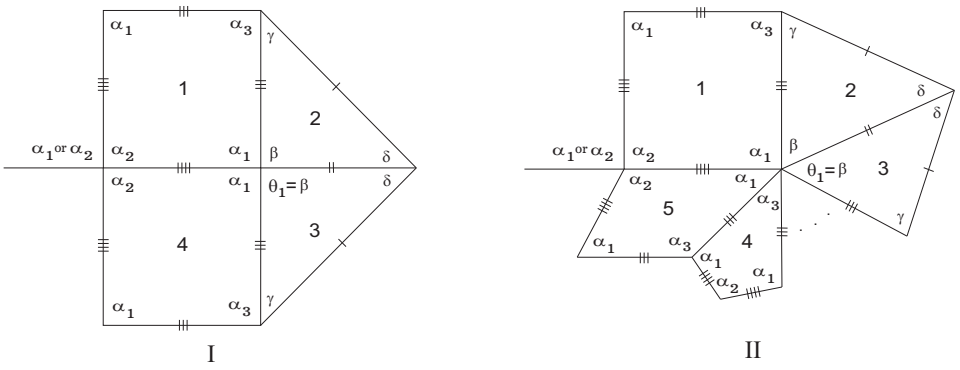

FIGURE 19. Local configurations

On the other hand, if $\alpha_1 < \gamma$, we get $\alpha_2+\beta > \alpha_2+\gamma > \alpha_2+\alpha_1 > \pi$, which is a contradiction. Observe that the indicated angle in tile 4 (cf. Figure 20-I) cannot be α_1, as two angles α_2 in adjacent positions are not allowed.

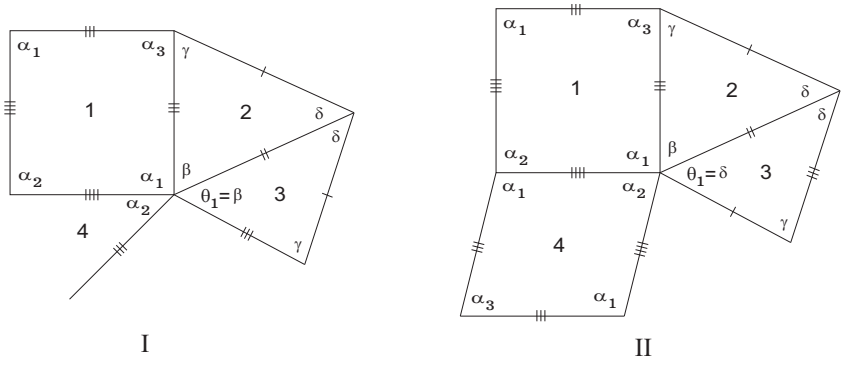

FIGURE 20. Local configurations

SUBCASE 1.2.2: $\alpha_3 > \alpha_1$:
Suppose now that $\alpha_3 > \alpha_1$, i.e., $\alpha_2 > \alpha_3 > \alpha_1$. It follows that the alternating sum containing β (tile 2 of Figure 18-II) satisfy $\beta + \alpha_2 < \pi$; however, then $\beta + \alpha_2 + \rho > \pi$ for any $\rho \in \{\alpha_1, \alpha_2, \alpha_3, \beta, \gamma, \delta\}$, which is a contradiction.

CASE 2: $\theta_1 = \delta$:
Assume finally that $\theta_1 = \delta$ (cf. Figure 18-II). Then we must have $\alpha_1 + \delta = \pi$ or $\alpha_1 + \delta < \pi$.

SUBCASE 2.1: $\alpha_1 + \delta = \pi$:
If $\alpha_1 + \delta = \pi$, then this forces an incompatibility between sides.

SUBCASE 2.2: $\alpha_1 + \delta < \pi$:
If $\alpha_1 + \delta < \pi$, then the sum of alternate angles containing β in tile 2 must satisfy $\alpha_2 + \beta + k\alpha_3 = \pi$ for some $k \geq 1$ (cf. Figure 20-II). However, when we take the edge lengths into account, we find that we have no way to set up the angles α_3. □

3. CASE OF ADJACENCY II

In this section we consider that any f-tiling using K and T has at least two cells congruent, to K and T, respectively, such that the cells are in adjacent positions as illustrated in Figure 2-II.

Upon considering the internal angles of the kite K, we have necessarily one of the following situations:

$$\alpha_1 \geq \alpha_2 > \alpha_3 \quad \text{or} \quad \alpha_2 > \alpha_1, \alpha_3;$$

note that this includes the cases in which $\alpha_2 > \alpha_1 \geq \alpha_3$ and $\alpha_2 > \alpha_3 > \alpha_1$.

The two propositions that follow address these distinct cases.

Proposition 3.1. *If $\alpha_1 \geq \alpha_2 > \alpha_3$, then there is an f-tiling using K and T if and only if*

$$\alpha_1 + \gamma = \pi, \quad \alpha_2 = \frac{\pi}{2}, \quad 2\beta + \alpha_3 = \pi \quad \textit{and} \quad \delta = \frac{\pi}{3}.$$

In this situation, there exists a continuous family of f-tilings, say $\mathcal{U}_\gamma$, with $\gamma \in (\gamma_{\min}, \gamma_{\max})$, where

$$\gamma_{\min} = \frac{\pi}{3} = 60^\circ$$

and

$$\gamma_{\max} = \arccos\sqrt{\frac{2}{11}} \approx 64.76^\circ.$$

Proof. Suppose that any f-tiling using K and T has at least two cells congruent, to K and T, respectively, such that the cells are in adjacent positions as illustrated in Figure 2-II and $\alpha_1 \geq \alpha_2 > \alpha_3$ with $\alpha_1 > \pi/2$.

As in Section 2, it follows that we cannot have two angles α_3 in adjacent positions; see Figure 3-I.

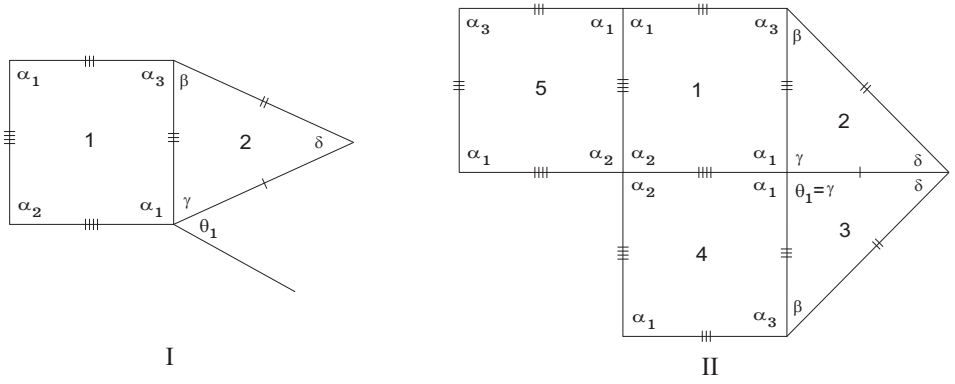

FIGURE 21. Local configurations

With the labeling of Figure 21-I, it follows that we necessarily have

$$\theta_1 = \gamma \qquad \text{or} \qquad \theta_1 = \delta.$$

This leads us to consider the following cases:

CASE 1: $\theta_1 = \gamma$:

Suppose firstly that $\theta_1 = \gamma$. Then we have $\alpha_1 + \gamma = \pi$ or $\alpha_1 + \gamma < \pi$.

SUBCASE 1.1: $\alpha_1 + \gamma = \pi$:

If $\alpha_1 + \gamma = \pi$, then $\alpha_1 > \pi/2 > \gamma$, we obtain the local configuration illustrated in Figure 21-II. Taking into account the side lengths and assuming that $\alpha_1 + \alpha_2 > \pi$, we obtain

$$\alpha_2 = \frac{\pi}{k}, \quad \text{for some } k \geq 2.$$

Moreover, as two angles α_3 in adjacent positions are not allowed, at vertices surrounded by the cyclic sequence $(\alpha_3, \beta, \dots)$ we get $2\beta + \alpha_3 = \pi$. Such information leads us to the configuration illustrated in Figure 22-I.

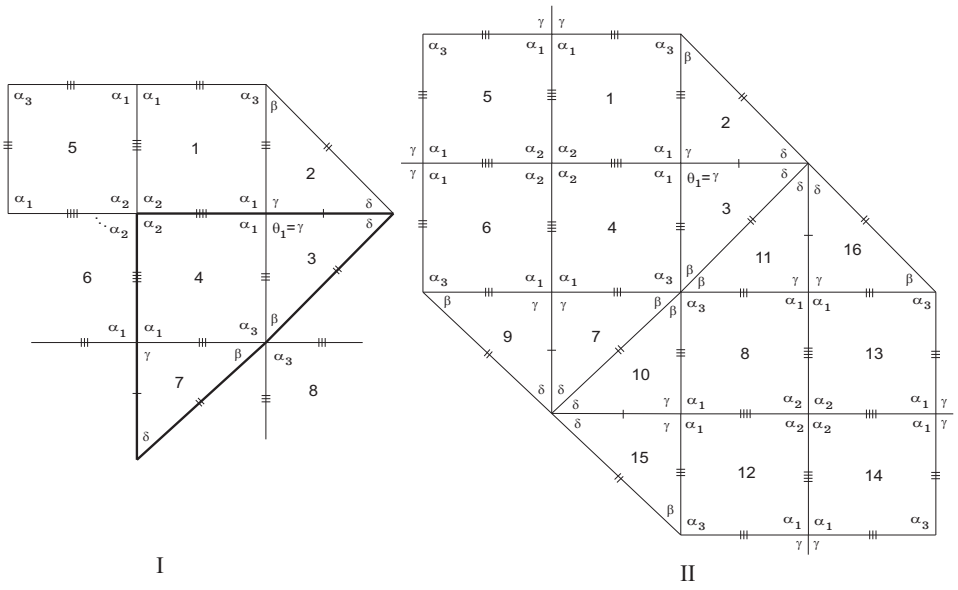

FIGURE 22. Local configurations

Considering the area of the bold triangle, composed by tiles 3, 4 and 7, we achieve $\alpha_2 + 2\delta - \pi > 0$, which means that $\pi/k + 2\delta > \pi$, or

$$\delta > \frac{k-1}{2k}\pi.$$

Now, if $k \geq 3$, then $\delta > \pi/3$. However, we then have that

$$\delta < \gamma < \alpha_2 = \frac{\pi}{k} \leq \frac{\pi}{3},$$

which is an impossibility. Thus $k = 2$, i.e.,

$$\alpha_2 = \frac{\pi}{2} \quad \text{and} \quad \delta > \frac{\pi}{4},$$

which allows us to extend our local configuration a little further. It follows that tiles adjacent to tile 8, say 12 and 13, must be kites (according to the edge lengths). As $\alpha_1 + \alpha_2 > \pi$, they are completely determined as shown in Figure 22-II. From now on, we easily obtain $\delta = \pi/3$ and hence there is a unique way to extend this configuration, leading us to the planar representation illustrated in Figure 9 with angles β and γ, and the corresponding sides, interchanged .

As before, we get $a + c + d = \pi/2$ and, concerning the distinct types of vertices, we have

$$\alpha_1 + \gamma = \pi \text{ (24 vertices)}, \;\; 2\,\alpha_2 = \pi \text{ (6 vertices)},$$
$$2\beta + \alpha_3 = \pi \text{ (12 vertices)}, \text{ and } \; 3\,\delta = \pi \text{ (8 vertices)}.$$

We reach a new family of f-tilings with one continuous parameter, say $\mathcal{U}_\gamma$, which is an extension of the family found in Proposition 2.1. As before, the knowledge of α_2 and δ allows to determine the extended triangle illustrated in Figure 23-I.

We now exhibit $\gamma_{\min}$ and $\gamma_{\max}$ such that for all $\gamma \in (\gamma_{\min}, \gamma_{\max})$ we get $\alpha_1 + \gamma = \pi$, $2\beta + \alpha_3 = \pi$, and Equation (1.1) is satisfied with $\beta > \gamma > \pi/3$.

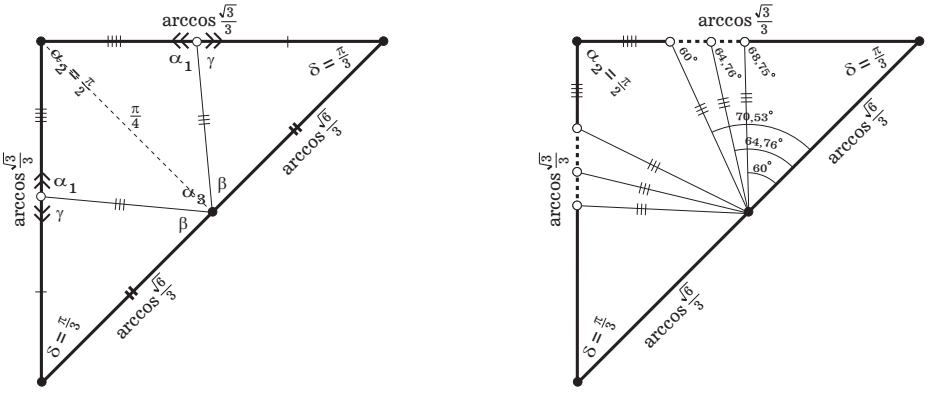

FIGURE 23. Extended triangles

Because γ increases if and only if β decreases, as seen in Proposition 2.1, we have that

$$\gamma_{\max} = \arccos\sqrt{\frac{2}{11}} \approx 64.76^\circ,$$

the value for which the triangle is isosceles ($\gamma = \beta$); this is the case studied in [**?**]. On the other hand, since $\gamma > \delta$ we obtain

$$\gamma_{\min} = \frac{\pi}{3} = 60^\circ,$$

as represented in Figure 23-II.

In order to determine the corresponding angle $\beta = \beta_{\max}$ for which $\gamma = \gamma_{\min} = \pi/3$, we proceed as follows: Consider the spherical isosceles triangle with angles $(\beta_{\max}, \pi/3, \pi/3)$ and edge lengths $\arccos\sqrt{6}/3$ (opposite to $\pi/3$) and c (opposite to $\beta_{\max}$), as represented in Figure 24-I. Using spherical trigonometry formulas, we derive that

$$\cos c = \cos^2\left(\arccos\frac{\sqrt{6}}{3}\right) + \sin^2\left(\arccos\frac{\sqrt{6}}{3}\right)\cos\beta_{\max}$$

and

$$\cos\beta_{\max} = -\cos^2\frac{\pi}{3} + \sin^2\frac{\pi}{3}\cos c,$$

which implies that $\cos c = 7/9$ and $\cos\beta_{\max} = 1/3$. Therefore it follows that (cf. Figure 23-II)

$$\beta_{\max} = \arccos\frac{1}{3} \approx 70.53^\circ.$$

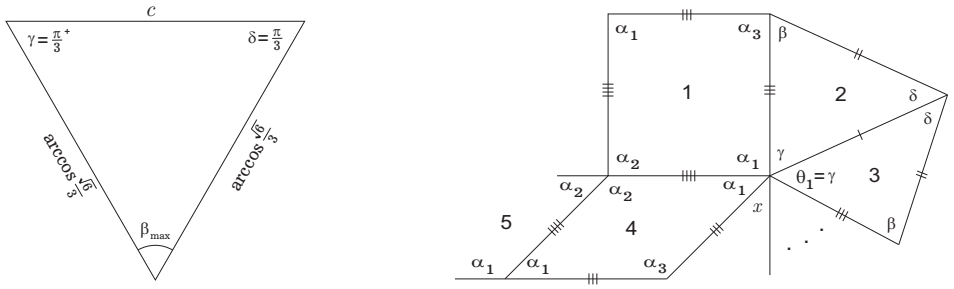

I II

FIGURE 24. An isosceles triangle / Local configuration

SUBCASE 1.2: $\alpha_1 + \gamma < \pi$:
If $\alpha_1 + \gamma < \pi$, we get the local configuration illustrated in Figure 24-II; observe that the tile labeled by 4 must be a kite and, by considering the edge lengths, it has a unique way of being positioned. With the labeling of this figure, we may conclude that $x = \alpha_3$ or $x = \gamma$.

SUBCASE 1.2.1: $x = \alpha_3$:
Suppose firstly that $x = \alpha_3$ (cf. Figure 25-I). As $2\alpha_1 > \pi$, tile 7 cannot be a kite. Hence, it is a triangle and its angles have a unique way of being positioned, since the case of adjacency I has already been studied and no f-tilings were obtained under these conditions. On the other hand, the indicated angle in tile 8 must be γ since two angles α_3 in adjacent positions lead to a contradiction. However, this gives

$$2\pi = (\alpha_1 + \beta + \dots) + (\alpha_1 + 2\gamma + \dots) \geq (\alpha_1 + \alpha_1) + (\beta + 2\gamma) > 2\pi,$$

which is a contradiction.

SUBCASE 1.2.2: $x = \gamma$:
Suppose that $x = \gamma$ (cf. Figure 25-II). Then we must have $\alpha_1 + 2\gamma + \dots = \pi$, and so $\beta > \alpha_1 > \pi/2$. It then follows immediately that tile 7 cannot be a kite nor a triangle, which is an impossibility.

CASE 2: $\theta_1 = \delta$:
Assume now that $\theta_1 = \delta$ (cf. Figure 21-I). We then have $\alpha_1 + \delta = \pi$ or $\alpha_1 + \delta < \pi$.

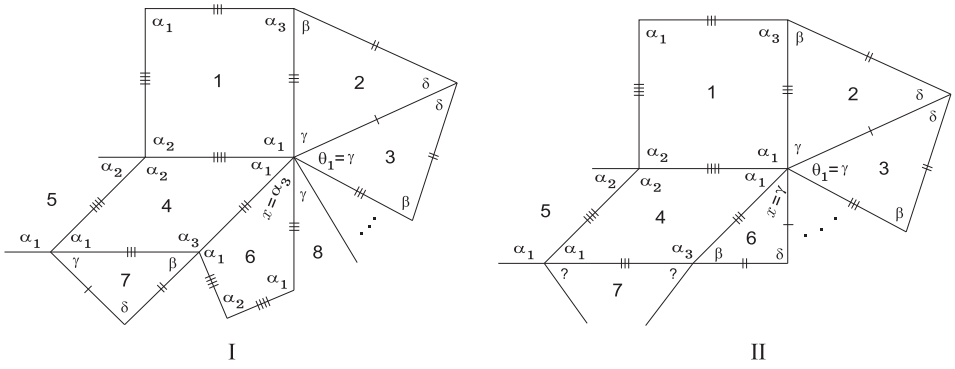

FIGURE 25. Local configurations

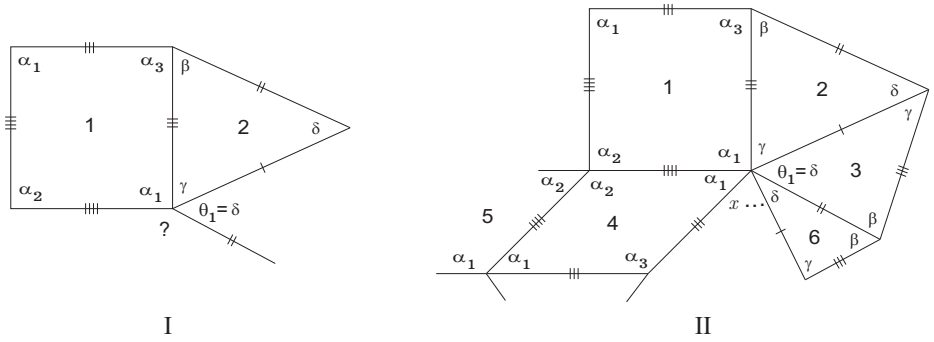

FIGURE 26. Local configurations

SUBCASE 2.1: $\alpha_1 + \delta = \pi$:
If $\alpha_1 + \delta = \pi$ (Figure 26-I), then it follows by analyzing the edge lengths that the sum of alternate angles containing γ cannot be formed.

SUBCASE 2.2: $\alpha_1 + \delta < \pi$:
The case $\alpha_1 + \delta < \pi$ is similar to the subcase 1.2 (i.e, it is similar to the case in which $\alpha_1 + \gamma < \pi$), and is illustrated in Figure 26-II. Observe that, with the labeling of this figure, one must have $x = \alpha_3$ or $x = \gamma$, which leads to a contradiction in each case. □

Proposition 3.2. *If $\alpha_2 > \alpha_1, \alpha_3$, then there is no f-tiling using K and T.*

Proof. Suppose that any f-tiling using K and T has at least two cells congruent to K and T, respectively, such that the cells are in adjacent positions as illustrated in Figure 2-II with $\alpha_2 > \alpha_1, \alpha_3$ and $\left(\alpha_2 > \frac{\pi}{2}\right)$.

Similarly to Proposition 2.2, we claim that there cannot be two angles α_2 in adjacent positions; see Figure 18-I.

It then follows that, with the labeling of Figure 21-I, we necessarily have

$$\theta_1 = \gamma \qquad \text{or} \qquad \theta_1 = \delta.$$

This leads us to consider the following cases:

Case 1: $\theta_1 = \gamma$

Assume firstly that $\theta_1 = \gamma$. Since the case $\alpha_1 + \gamma = \pi$ leads to two angles α_2 in adjacent positions, we must have $\alpha_1 + \gamma < \pi$.

In this case, we get the local configuration illustrated in Figure 27-I. Furthermore, observe that tiles labeled by 4 and 5 must be kites; considering that there cannot be two angles α_2 in adjacent positions, these tiles have a unique way of being positioned. Now, as $2\alpha_1 + \alpha_2 + \alpha_3 > 2\pi$ and $(\alpha_1 + \alpha_2) + (\beta + 2\gamma) > 2\pi$, none of the angles around vertex v could be α_3 or β. By this reason, the remaining angles around v must be γ's and δ's. When taking taking into account the edge lengths, we see that there is no way to avoid an incompatibility.

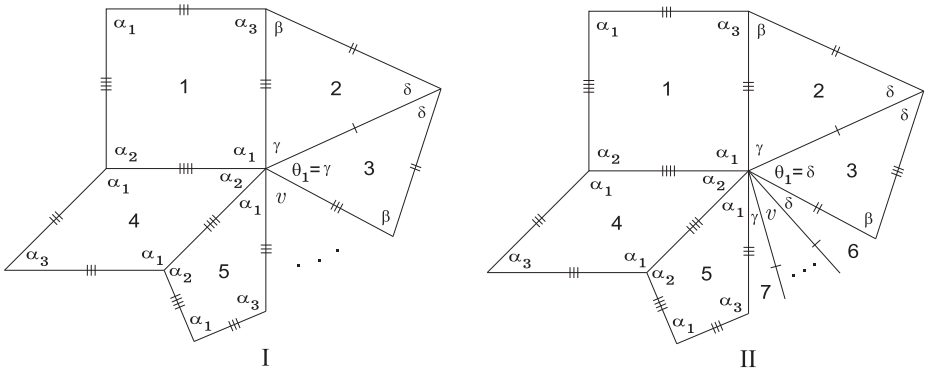

Figure 27. Local configurations

Case 2: $\theta_1 = \delta$:

Suppose now the case in which $\theta_1 = \delta$. The case $\alpha_1 + \delta = \pi$ leads to a contradiction (similar to the same case in Proposition 3.1), and so we suppose that $\alpha_1 + \delta < \pi$ (cf. Figure 27-II). As before, tiles labeled by 4 and 5 are uniquely determined, while none of the angles around vertex v can be α_3 or β. This implies that tiles labeled by 6 and 7 are triangles positioned as shown in Figure 27-II. Nevertheless, when taking into account the edge lengths, we find that we have no way to complete the sum of alternate angles around the vertex v. □

4. Conclusion

Let K be a spherical kite with internal angles $(\alpha_1, \alpha_2, \alpha_1, \alpha_3)$ in cyclic order such that $\alpha_2 > \alpha_3$. Let T be a scalene spherical triangle with internal

angles (β, γ, δ) such that $\beta > \delta$, $\gamma > \delta$ and $\beta \neq \gamma$. For each

$$\beta \in \left(\frac{\pi}{3}, \arccos \frac{\sqrt{6}-1}{4} \right) \setminus \left\{ \arccos \sqrt{\frac{2}{11}} \right\},$$

there is exactly one f-tiling of the sphere, $\mathcal{U}_\beta$, with prototiles K and T in which the longer side of K matches the shortest side of T satisfying

$$\alpha_1 + \beta = \pi, \quad \alpha_2 = \frac{\pi}{2}, \quad 2\gamma + \alpha_3 = \pi, \quad \text{and} \quad \delta = \frac{\pi}{3};$$

for other values of β no such tiling exists. Moreover, given β in the specified interval, the angle γ is uniquely determined by Equation (1.1). In fact, $\gamma \in (\pi/3, \arccos(1/3))$, and γ decreases if and only if β increases. The case $\beta = \arccos\sqrt{2/11}$ implies $\beta = \gamma$, and hence must be excluded. A 3D representation of U_β is illustrated in Figure 11-II.

The symmetries of $\mathcal{U}_\beta$ that fix a vertex v of valency four and surrounded by $(\alpha_2, \alpha_2, \alpha_2, \alpha_2)$ are generated by a reflection and by a rotation through an angle $\pi/2$ around the axis by $\pm v$. On the other hand, for any vertices v_1 and v_2 of this type, there is a symmetry of $\mathcal{U}_\beta$ sending v_1 into v_2. It follows that the symmetry group has exactly $48 = 6 \cdot 8$ elements, and it forms the group of all symmetries of the cube, the octahedral group, often referred to as $C_2 \times S_4$.

References

[1] C. P. Avelino and A. F. Santos, *Spherical and planar folding tessellations by kites and equilateral triangles*, Australas. J. Combin. **53** (2012), 109–125.

[2] ———, *Spherical folding tesselations by kites and isosceles triangles ii*, Int. J. Pure. Appl. Math. **85** (2013), no. 1, 45–67.

[3] ———, *Spherical folding tessellations by kites and isosceles triangles: a case of adjacency*, Math. Commun. **19** (2014), no. 1, 1–28.

[4] ———, *Spherical folding tessellations by kites and isosceles triangles IV*, Ars Math. Contemp. **11** (2016), no. 1, 59–78.

[5] A. M. Breda, *A class of tilings of S^2*, Geom. Didicata **44** (1992), no. 3, 241–253.

[6] A. M. Breda and P. S. Ribeiro, *Spherical f-tilings by two non-congruent classes of isosceles triangles—I*, Math. Commun. **17** (2012), no. 1, 127–149.

[7] A. M. Breda, P. S. Ribeiro, and A. F. Santos, *A class of spherical dihedral f-tilings*, European J. Combin. **30** (2009), no. 1, 119–132.

[8] A. M. Breda and A. F. Santos, *Dihedral f-tilings of the sphere by rhombi and triangles*, Discrete Math. Theor. Comput. Sci. **7** (2005), no. 1, 123–141.

[9] R. J. Dawson, *Tilings of the sphere with isosceles triangles*, Discrete Comput. Geom. **30** (2003), no. 3, 467–487.

[10] R. J. Dawson and B. Doyle, *Tilings of the sphere with right triangles. I. The asymptotically right families*, Electron. J. Combin. **13** (2006), no. 1, Research Paper 48, 31.

[11] ———, *Tilings of the sphere with right triangles. II. The $(1, 3, 2), (0, 2, n)$ subfamily*, Electron. J. Combin. **13** (2006), no. 1, Research Paper 49, 22.

[12] S. A. Robertson, *Isometric folding of Riemannian manifolds*, Proc. Roy. Soc. Edinburgh Sect. A **79** (1978), no. 3-4, 275–284.

[13] Y. Ueno and Y. Agaoka, *Classification of tilings of the 2-dimensional sphere by congruent triangles*, Hiroshima Math. J. **32** (2002), no. 3, 463–540.

CMAT-UTAD, CEMAT-IST-UL, Universidade de Trás-os-Montes e Alto Douro, UTAD, Vila Real, Portugal
E-mail address: cavelino@utad.pt

CMAT-UTAD, Universidade de Trás-os-Montes e Alto Douro, UTAD, Vila Real, Portugal
E-mail address: afolgado@utad.pt